

SEISMIC PERFORMANCE-BASED DESIGN OF OFFSHORE FOUNDATIONS: INSIGHTS FROM PREDICTIVE MODEL AND FRAGILITY CURVES

Ali Lashgari

Department of the Built Environment, Aalborg University, Aalborg, Denmark, Email: alil@build.aau.dk

Amin Barari

*Department of the Built Environment, Aalborg University, Aalborg, Denmark, Email: abar@build.aau.dk
& School of Engineering, RMIT University, Melbourne, Australia, Email: amin.barari@rmit.edu.au*

Jannie Sønderkær Nielsen

Department of the Built Environment, Aalborg University, Aalborg, Denmark, email: jsn@build.aau.dk

This study evaluates the role of effective factors on the seismic performance of offshore wind turbines supported by suction caisson foundation using probabilistic analysis. The probabilistic analyses incorporate data and the predictive models developed by the second author to estimate liquefaction-induced settlement in these structures. Fragility curves and surfaces are developed to assess the probability of exceeding settlement limit states under varying seismic conditions. The analysis considers key factors such as contact pressure (Q) and shaking intensity rate (SIR). The results indicate that Q and SIR can significantly influence the probability of settlement damage. However, sensitivity analyses demonstrated that the settlement probability is more sensitive to variations in SIR compared to Q . Moreover, fragility surfaces highlighted the multivariate nature of settlement probability based on the combination of Q and SIR effects. The proposed fragility surfaces can provide valuable insights for the design and seismic risk assessment of suction caisson foundations in offshore wind farms.

Keywords: Fragility curves; Probabilistic analysis; Offshore wind turbine; Suction caisson foundations

1. Introduction

The global expansion of offshore wind energy has amplified the demand for suitable sites where wind farms can efficiently generate power. Many potential locations lie in seismically active regions, where seismic hazards pose significant risks to the stability and operational performance of offshore wind turbines (OWTs). Seismic hazards including site response, fault rupture, submarine landslides, and soil liquefaction can affect the performance of OWTs (e.g., Bhattacharya 2019). A typical offshore wind farm consists of multiple interconnected components all of which must remain operational following seismic events. This necessitates a comprehensive design for seismic resilience (e.g., Bhattacharya et al., 2021).

Over the past two decades, the performance-based seismic design concept has gained prominence, focusing on the prediction of the structures and geosystems performance under seismic loading (e.g., Kramer 2014). Recent standards emphasize hazard and risk assessment for seismic design that require predictive models and fragility curves for estimating the system performance. However, there has been limited research into the performance of OWTs under seismic hazards. Farahani and Barari (2024) investigated shear-induced soil-structure interaction mechanisms through effective stress analyses of caisson-supported OWTs on uniform sand deposits, evaluating contact pressures and ground motion characteristics. They proposed simplified predictive models based on statistical and machine-learning techniques.

Fragility curves have emerged as valuable tools in performance-based design and seismic risk assessment that can provide an estimation of the failure probability of geosystems. However, widely applied to ground structures such as buildings and dams (e.g., Fotopoulou and Pitilakis 2013; Lashgari and Moss, 2024), their application to offshore foundations remains underexplored. Recent studies have developed fragility curves for offshore wind turbines subjected to aerodynamic loading (e.g., Zuo et al., 2023). However, further fragility analyses are still required to consider other triggering mechanisms including seismic loading and soil liquefaction. Despite advancements in fragility assessment for structures, the estimation of fragility curves for offshore foundations is a critical research gap.

This study presents fragility curves for caisson-supported wind turbines by evaluating the effects of key factors such as Q on intensity measures (IMs). The study includes two main parts (1) presenting the details of the suction caisson foundation and the proposed liquefaction-induced settlement predictive model; (2) performing the probabilistic and fragility analyses to develop fragility curves by considering variations of IM and Q . Moreover, the impacts of key factors on the settlement probability will be discussed using a sensitive analysis. Finally, the fragility surfaces are represented to illustrate the combined influence of these key parameters.

2. Suction caisson foundations and settlement predictive model

As shown in Fig. 1(a) the major offshore wind farm developments together with the global seismic hazard map. This shows that all types of OWT foundations are exposed to seismic hazards. OWTs utilize various foundation types including gravity foundations to jacket foundations, depending on the water depth. As illustrated in Fig. 1(c),

suction caissons are an optimal choice for mid-depth waters, typically around 30 meters. A suction caisson-supported OWT system comprises three main sections: the hub, the tower, and the caisson foundation as depicted in Fig. 1(b). Farahani and Barari (2023) developed a nonlinear finite-element model to simulate the seismic behaviour of OWTs supported by caisson foundations. The domain configuration and mesh generation for the numerical analysis were shown in Fig. 1(d). Following validation of the numerical model against centrifuge test results, they performed several analyses using 20 different seismic ground motions.

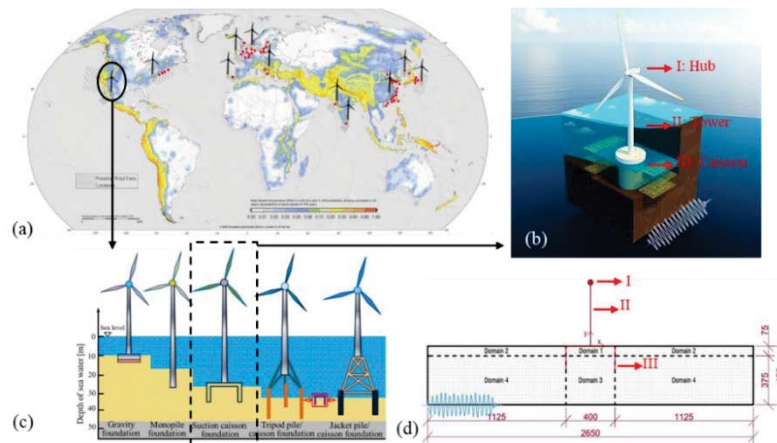


Fig. 1.(a) locations of planned OWTs and seismic zones (Bhattacharya et al., 2021) (b) details of suction caisson foundation (c) different types of OWT foundations (after Li et al. 2024) (d) domain distribution and mesh generation for numerical analysis (after Farahani and Barari 2024)

Farahani and Barari (2023) proposed predictive models for estimating the settlement of suction caisson foundations subjected to liquefaction-induced deformation based on statistical and machine-learning analyses. Accordingly, the settlement was expressed as a function of IM and Q using the following equation:

$$S_{OWT} = c_1 + c_2IM + c_3Q + c_4IM^2 + c_5IMQ + c_6Q^2 + c_7IM^3 + c_8IM^2Q + c_9IMQ^2 \quad (1)$$

where S_{OWT} , $c_{1...9}$, IM , and Q are foundation settlement, constant factors that change based on used IM , intensity measure, and contact pressure. They indicated that the SIR parameter (ratio between Arias Intensity and Duration) can provide reasonable results compared to other IMs such as peak ground acceleration. The SIR incorporates the effects of the interaction between the suction caisson, foundation soil, excess pore-pressure generation, and cyclic shear stresses. It is noted that they suggested using the model with caution at low SIR values (<0.08) due to the presence of bias, which could affect its reliability in these scenarios. The proposed predictive model reasonably incorporates the relative importance of key site properties, the structure and characteristics of the earthquake motion, the effects of the interaction between the caisson foundation and relatively thin liquefiable seabed, and the generation of excess pore-pressure. Moreover, the proposed model was validated by numerical modelling results and centrifuge model test data. The predictive model provides useful insights into the complex phenomena governing the deviatoric component of the settlement of offshore foundations. For further details, refer to Farahani and Barari (2023).

3. Fragility analysis

Seismic fragility curves are widely utilized to assess the vulnerability of structures and geo-systems to earthquake-induced damage. These curves represent the probability of failure as a function of IMs and serve as critical tools for seismic design and risk assessment. Engineers derive fragility curves using two primary methods: (1) predictive models (e.g., Pitilakis et al., 2014); or (2) direct integration of sliding displacement data without relying on predefined regression models (e.g., Jafarian et al., 2021). Fragility curves estimate the probability that a specific engineering demand parameter exceeds a predefined limit state (LS) under seismic loading characterized by a given IM . In this study, the seismic settlement of suction caisson foundations is selected as the demand parameter, with shaking intensity described by IM . The fragility curve is derived based on the probabilistic distribution of settlement, expressed as follows:

$$P[S_{OWT} \geq LS | IM] = 1 - \Phi \left(\frac{\ln(LS) - \ln(S_{OWT})}{\sqrt{\sigma_{LnD}^2 + \sigma_{LnLS}^2}} \right) \quad (2)$$

where $\Phi(\cdot)$ is the standard lognormal cumulative distribution function, σ_{LnD} is the standard deviation of the predictive model (scalar or vector), σ_{LnLS} is the standard deviation of limit states that were assumed 15% of LS

displacement for each LS (Jafarian et al. 2021). It is important to note that specific settlement LS for suction caisson foundations corresponding to different damage states are not explicitly defined in existing guidelines. However, these structures are typically designed based on an ultimate limit state (ULS) that is defined as a maximum settlement equal to 10% of the foundation diameter (Barari et al. 2017). In this study, this criterion was employed as the ULS. Moreover, two other settlement thresholds corresponding to 2.5% and 5% of the diameter were considered for low and intermediate LS values. Given that the diameter of the suction caisson model used in this study is 4 m, the maximum settlement thresholds were determined to be approximately 10 cm, 20 cm, and 40 cm for the 2.5%, 5%, and 10% criteria, respectively.

3.1. Fragility curve

Figure 2 shows the variations in the probability of exceedance from LS s of 20 cm and 40 cm, plotted against SIR with varying Q . As Fig. 2(a) indicates, the probability of exceedance for $LS > 20$ cm remains below 10% for $SIR < 0.35$ across all values of Q . However, as SIR and Q increase, the probability rises significantly, reaching 78% for $Q=40$ kPa at $SIR=1$ m/s². Comparison between the variation of probabilities during the variations of Q reveals that the probability increases from 30% to 78% as Q increases from 7 kPa to 40 kPa. However, the influence of Q diminishes for values exceeding 30 kPa, with a marginal difference of only 4% observed. Comparing Figs. 2(a) and 2(b) shows a notable reduction in the probability of failure as the limit state increases from 20 cm to 40 cm. For instance, the probability of exceedance decreases to approximately 34% for $LS=40$ cm, $Q=40$ kPa, and $SIR=1$ m/s². This indicates that higher contact pressures ($Q > 30$ kPa) are more likely to result in settlements exceeding 20 cm, particularly under intense seismic conditions.

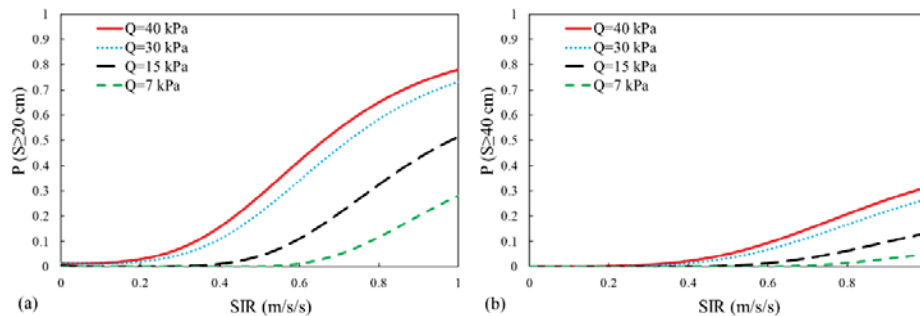


Fig. 2. Variations of the probability of exceedance from the LS versus SIR for (a) $LS=20$ cm (b) $LS=40$ cm

Figure 3 shows the probability of exceedance plotted against variations in Q for different SIR values. The sensitivity of probability to changes in SIR is notably higher than its sensitivity to Q . For instance, in Fig. 3(a), the probability increases significantly from 5% to 78% at $Q=40$ kPa as SIR rises from 0.25 to 1 cm/s². Moreover, a similar trend is observed for $LS=40$ cm in Fig. 3(b), with a 15% increase in probability corresponding to the same SIR variation. Comparison between Figs. 2 and 3 indicates that the probability of exceedance reduces when Q decreases, however, with a slower rate compared to changes in SIR . Physically, the probability should approach zero as Q approaches zero. This trend is generally observed for most SIR values; however, at $SIR=1$, the probability remains around 7%. This bias can be attributed to the parameter range limitations of the predictive model, which was developed using Q values between 7 and 40 kPa. Additionally, both Q and SIR significantly influence the probability of damage as illustrated in Figs. 2-3. This indicates that the settlement probability for caisson-supported foundations is inherently multivariate, depending on the combined effects of these parameters.

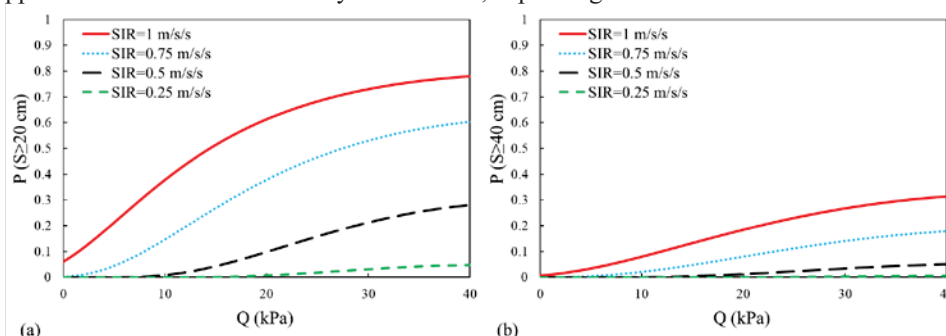


Fig. 3. Variations of the probability of exceedance from the LS versus Q for (a) $LS=20$ cm (b) $LS=40$ cm

3.2. Fragility surface

Figure 4 presents a 3D plot illustrating the variations in the probability of exceedance against SIR and Q for three LS s of 10, 20, and 40 cm. As shown in Fig. 4(a), the probability of exceedance exceeds 80% for all levels of Q at

LS=10cm when $SIR > 0.87$. Moreover, the probability decreases significantly with increasing LS; for instance, the probability drops from 100% to 50% at the maximum case as LS increases from 10 cm to 40 cm. This trend indicates that achieving a large settlement (i.e., LS=40cm) requires both higher seismic energy (e.g., SIR) and greater Q . This figure also shows that the threshold value of SIR corresponding to a 50% probability of exceedance from LS=10 cm is approximately 0.65 for $Q=10$ kPa and 0.35 for $Q=40$ kPa. However, these values can change for other LSs. This demonstrates the combined influence of SIR and Q in determining the probability of damage to suction caisson foundations. The fragility surfaces emphasize the importance of incorporating both parameters into a comprehensive seismic risk assessment for settlement, ensuring accurate and reliable evaluations.

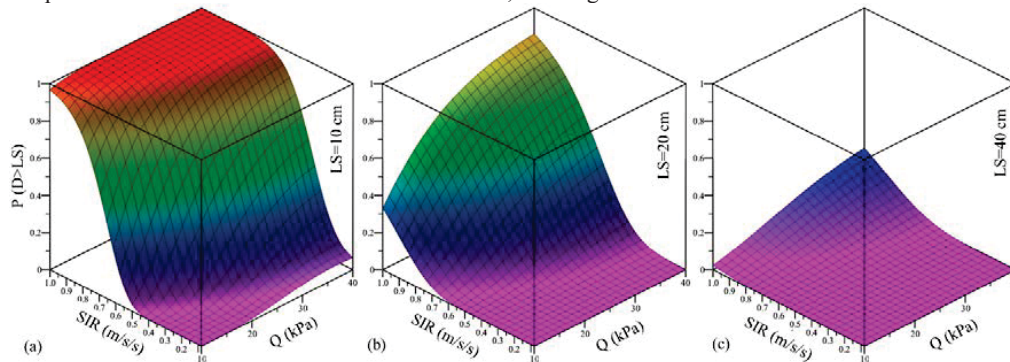


Fig. 4. The proposed fragility surfaces using combination on SIR and Q for (a) $LS=10$ cm (b) $LS=20$ cm (c) $LS=40$ cm

4. Conclusion

This study evaluated the seismic performance of suction caisson foundations supporting OWTs based on a predictive model using fragility analyses to estimate the probability of settlement-induced damage under varying SIR and Q values. The results show that the probability of exceeding settlement LS is more sensitive to variations in SIR than Q . Moreover, probabilities of exceedance decrease as the LS increases. For larger settlements (e.g., $LS=40$ cm), both higher SIR and Q are required to reach significant probabilities. This emphasizes the role of both seismic energy and foundation pressure in causing substantial damage. Additionally, a 50% probability of exceedance for low Q values corresponds to $SIR \approx 0.6 \text{ m/s}^2$, underscoring the importance of seismic energy thresholds in fragility analysis. The results reveal that the probability of settlement for suction caisson foundations is inherently multivariate, relying on the interaction between SIR and Q . This interaction was demonstrated through probability surfaces, showing the combined role of these parameters in driving damage probabilities.

These findings provide valuable insights for the design and seismic risk assessment of suction caisson foundations in offshore wind farms. Future work should aim to refine predictive models by expanding the parameter range and incorporating additional uncertainties to enhance the robustness of fragility analyses for these critical structures.

Acknowledgement

The research received support from the European Union under the Marie Skłodowska-Curie Postdoctoral Fellowships grant agreement No 101106129.

References

- Barari, A., Ibsen, L. B., Taghavi Ghalesari, A., & Larsen, K. A. (2017). Embedment effects on vertical bearing capacity of offshore bucket foundations on cohesionless soil. *International Journal of Geomechanics*, 17(4), 04016110.
- Bhattacharya, S. (2019). *Design of foundations for offshore wind turbines*. John Wiley & Sons.
- Bhattacharya, S., Biswal, S., Aleem, M., Amani, S., Prabhakaran, A., Prakhya, G., ... & Mistry, H. K. (2021). Seismic design of offshore wind turbines: good, bad and unknowns. *Energies*, 14(12), 3496.
- Farahani, S., & Barari, A. (2023). A simplified procedure for the prediction of liquefaction-induced settlement of suction caisson foundation based on effective stress analyses and an ML-based group method of data handling. *Earthquake Engineering & Structural Dynamics*, 52(15), 5072-5098.
- Fotopoulou, S. D., & Ptilakis, K. D. (2013). Fragility curves for reinforced concrete buildings to seismically triggered slow-moving slides. *Soil Dynamics and Earthquake Engineering*, 48, 143-161.
- Jafarian, Y., Lashgari, A., & Miraie, M. (2021). Multivariate fragility functions for seismic landslide hazard assessment. *Journal of Earthquake Engineering*, 25(3), 579-596.
- Kramer, S. L. (2014). Performance-based design methodologies for geotechnical earthquake engineering. *Bulletin of Earthquake Engineering*, 12, 1049-1070.
- Lashgari, A., & Moss, R. E. S. (2024). Displacement and damage analysis of earth dams during the 2023 Türkiye earthquake sequence. *Earthquake Spectra*, 40(2), 939-976.

- Li, D., Zhao, J., Wu, Y., Zhang, Y., and Liang, H. (2024). An innovative bionic offshore wind foundation: Scaled suction caisson. *Renewable and Sustainable Energy Reviews*, 191, 114208.
- Pitilakis, K., Crowley, H., & Kaynia, A. M. (2014). SYNER-G: typology definition and fragility functions for physical elements at seismic risk. *Geotechnical, Geological and Earthquake Engineering*, 27, 1-28.
- Zuo, H., Bi, K., Hao, H., Xin, Y., Li, J., & Li, C. (2020). Fragility analyses of offshore wind turbines subjected to aerodynamic and sea wave loadings. *Renewable Energy*, 160, 1269-1282.